L. A. Slobozhanin, M. Gomez, and J. M. Perales

Stability of Liquid Bridges Between Unequal Disks under Zero-gravity Conditions

The stability of axisymmetric equilibrium shapes of a liquid bridge between two coaxial disks of different radii under zero-gravity conditions is investigated. The stability regions have been calculated for different values of the ratio of the disk radii in terms of the dimensionless parameters which characterize the length and the volume of the bridge. It has been found that disk radii unequality radically changes the upper boundary of the stability region. The analysis of the shape of marginally stable equilibrium surfaces has been carried out. Relationships between the critical values of the parameters have been deduced for some particular cases, which are of special interest for the materials purification processes and growing of single crystals by the floating zone method: for typical values of the growing angle for semi-conductor materials and for liquid volumes close to that of the cylinder having a radius equal to the mean radius of the disks.

1 Introduction

The last years increasing interest in the study of equilibrium shapes of a liquid bridge between two circular coaxial disks and their stability is connected with the problems arising during the modeling of the process of purification of materials and growth of single crystals in space by the floating zone method [1, 2].

Presently, most of the investigations are connected with the most simple typical case, namely with axisymmetric equilibrium states, when a liquid mass of volume v forms an axisymmetric bridge between two coaxial disks of radii r_1 and r_2 ($r_1 \leq r_2$), which are spaced a distance l apart, and the gas-liquid-solid contact line is pinned to the edges of disks (fig. 1).

For zero-gravity conditions the problem of determining the equilibrium shapes and their stability has been solved almost completely only in the case when disks are of equal radius ($K \equiv r_1/r_2 = 1$). This study was initiated by the Belgium physicist *Plateau* who presented a qualitative description of his experimental results in a celebrated treatise [3] (see also [4]). *Gillette* and *Dyson* [5] investigated theoretically the stability of the equilibrium shapes with respect to axisymmetric perturbations and computed the boundary of the stable region in the plane of the two parameters characterizing the equilibrium of system: slenderness $\Lambda_1 = l/2r_1$ and relative liquid volume $V_1 \equiv v/(\pi r_1^2 l)$. Later, *Slobozhanin* [6] (see also [7]) investigated the stability of such system with respect to arbitrary (not necessarily axisymmetric) perturbations. Experimental data on the boundary of the stable region were obtained by *Sanz* and *Martinez* [8] and *Russo* and *Steen* [9].

The first results concerning with stability of liquid bridges between unequal disks were obtained by *Martinez* [10]. He determined the minimum possible volume of a stable liquid bridge (considering only axisymmetric perturbations) for a set values of $K \leq 1$ and he constructed part of the lower boundary (that corresponding to moderately large values of the slenderness) of the stable region in the plane of the dimensionless variables $\Lambda \equiv l/(r_1 + r_2)$ and $\bar{V} \equiv v/(r_1 + r_2)^3$.

More complete results on this have been published later by *Martinez* and *Perales* [11]. Here the dependence $\bar{V}(\Lambda)$ on the minimum volume stability limit has been calculated and tabulated for values $\Lambda \geq 0.6$ and different values of $K \leq 1$. Besides, the values of the parameters characterizing the shape of the corresponding neutrally stable equilibrium surfaces are presented. As a distinctive characteristic, for $\Lambda \geq 0.6$ and $0.1 \leq K \leq 1$ the critical shape are unduloids for the lower boundary. In addition, they determined the parameters of critical catenoidal surfaces for each considered value of K. Approximate formulas for the description of the dependence $\bar{V}(\Lambda, K)$ on the lower boundary in case of long liquid bridges and slightly unequal disks were deduced by *Meseguer* [12, 13].

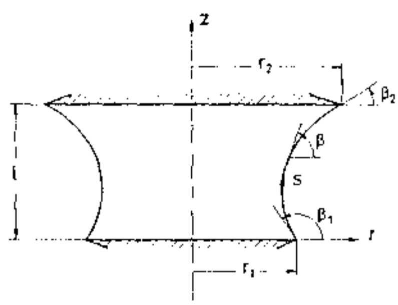

Fig. 1. Geometry and coordinate system for the liquid bridge problem

Mail address: Lev A. Slobozhanin, B. Verkin Institute for Low Temperature Physics and Engineering, Academy of Sciences of Ukraine, 47 Lenin Ave., 310164 Kharkov, Ukraine, Mariola Gomez, Jose M. Perales, Lamf/ETSI Aeronáuticos, UPM, Ciudad Universitaria, E-28040 Madrid, Spain.
Paper submitted: May 13, 1994
Paper accepted: October 21, 1994

This paper aims to construct the general boundary of the stable region for a wide range of values of the parameter K. The minimum permissible volume (the lower boundary of stability region) will be determined not only in case of critical unduloidal and catenoidal surfaces, but also for nodoidal surfaces (corresponding to small values of Λ). Besides, it is necessary to construct the upper boundary of the stability region which determines the maximum permissible volume for axisymmetric bridges. The stability will be studied with respect not only to axisymmetric perturbations, but to arbitrary ones.

These boundaries, constructed for various values of K in the plane of parameters (Λ, $V \equiv 4v/[\pi(r_1 + r_2)^2 l]$), together with certain characteristics of the shape of the neutrally stable equilibrium surfaces (namely, the values of angles β_1 and β_2 on the smaller and the larger disk, see fig. 1) allow to find the critical values of the parameters for fixed values of V, β_1, or β_2. Nevertheless, the critical values of liquid bridge parameters for values of V close to 1 as well as for constant values of angles β_1 and β_2, which have the special interest in the floating zone technology, will be presented.

2 Solution Methods

We shall assume for the sake of definiteness that the larger disk is above the smaller one. Let us place the origin of the cylindrical system of coordinates (r, θ, z) at the center of the smaller disk and let us point the z-axis towards the larger disk (fig. 1). The shape of an axisymmetric equilibrium free surface in the parametric form $r(s)$, $z(s)$ (s is the arc length of any meridian section $\theta = const.$) is described by the solutions of the following equations [7]:

$$r'' = -z'\left(q - \frac{z'}{r}\right), \quad z'' = r'\left(q - \frac{z'}{r}\right), \quad \left(' \doteq \frac{\mathrm{d}}{\mathrm{d}s}\right),$$

where q is twice the mean curvature of the surface.

For any non-catenodial surface ($q \neq 0$), the transformation

$$\varrho = |q|r, \quad \zeta = |q|z, \quad \tau = |q|s$$

leads to the system

$$\varrho'' = -\zeta'\beta', \tag{1a}$$

$$\zeta'' = \varrho'\beta', \tag{1b}$$

$$\beta' = \pm 1 - \frac{\zeta'}{\varrho}, \qquad \left(' \doteq \frac{\mathrm{d}}{\mathrm{d}\tau}\right). \tag{1c}$$

Here $\beta = \beta(\tau)$ is the angle between the ϱ-axis and the tangent to the equilibrium profile (the surface axial section) which is directed in the sense of increasing τ. The upper (lower) sign in eq. (1c) corresponds to a positive (negative) value of q.

The solution of the system of eqs. (1) is sought under the following initial conditions on the smaller disk:

$$\varrho(0) = \varrho_1, \quad \varrho'(0) = \cos(\beta_1), \quad \zeta(0) = 0, \quad \zeta'(0) = \sin(\beta_1),$$

$$\beta(0) = \beta_1. \tag{2}$$

According to the method described in [7], to determine the critical (neutrally stable) equilibrium surface the following problems which determine the functions $\varphi_{01}(\tau)$, $\varphi_{02}(\tau)$ and $\varphi_1(\tau)$ must be solved together with the problem (1)–(2):

$$\varphi''_{01} + \frac{\varrho'}{\varrho}\varphi'_{01} + \left(\beta'^2 + \frac{\zeta'^2}{\varrho^2}\right)\varphi_{01} = 0, \qquad \varphi_{01}(0) = 0, \quad \varphi'_{01}(0) = 1,$$

$$\varphi''_{02} + \frac{\varrho'}{\varrho}\varphi'_{02} + \left(\beta'^2 + \frac{\zeta'^2}{\varrho^2}\right)\varphi_{02} + 1 = 0, \quad \varphi_{02}(0) = 0, \quad \varphi'_{02}(0) = 1,$$

$$\varphi''_1 + \frac{\varrho'}{\varrho}\varphi'_1 + \left(\beta'^2 - \frac{\varrho'^2}{\varrho^2}\right)\varphi_1 = 0, \qquad \varphi_1(0) = 0, \quad \varphi'_1(0) = 1.$$

The integration of the systems should proceed up to the point $\tau = \tau_* > 0$ where either the function $\varphi_1(\tau)$ or the function

$$D(\tau) \equiv -\varphi_{01}(\tau)\int_0^{\tau} \varrho\varphi_{02}\,\mathrm{d}\tau + \varphi_{02}(\tau)\int_0^{\tau} \varrho\varphi_{01}\,\mathrm{d}\tau$$

vanish for the first time. Since, for a given value of K and a chosen value of β_1, the quantity $\varrho(\tau_*)$ depends on ϱ_1, the quantity ϱ_1 must be changed until we obtain, for some $\varrho_1 = \varrho_1^0$, a value $\tau_*^0 = \tau_*(\varrho_1^0)$ such that the condition

$$\varrho(\tau_*^0) = \frac{1}{K}\varrho_1$$

is satisfied within the required accuracy (checking that, for this value, $\zeta(\tau_*^0) > 0$). For a given value of K, there exists an interval of values of β_1, for which the above problem has a solution.

For the obtained value $\varrho_1 = \varrho_1^0$, the solution of the problem (1)–(2) on the interval $0 \leq \tau \leq \tau_*^0$ determines the shape of the profile of the neutrally stable equilibrium surface (if this profile does not intersect the disks surface at some interior point τ, $0 < \tau < \tau_*^0$). This surface is critical with respect to axisymmetric perturbations if the function which

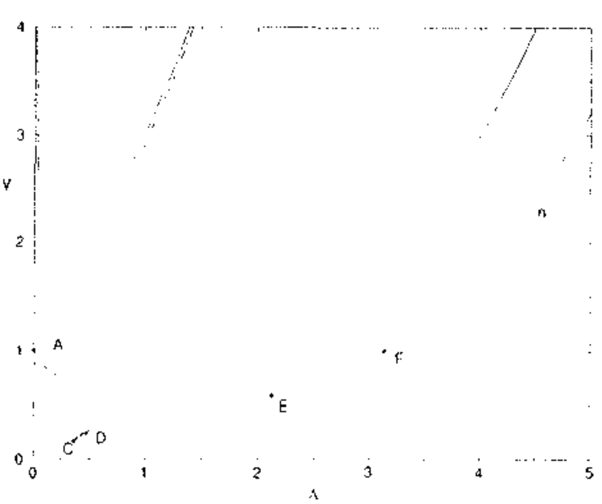

Fig. 2. Upper and lower boundaries of stability region of liquid bridges with a disk radii ratio of $K = 0.7$ (solid lines) and $K = 1$ (dot-dash lines). The points A, C, D, E and F show relevant changes in the behaviour in the case $K = 1$

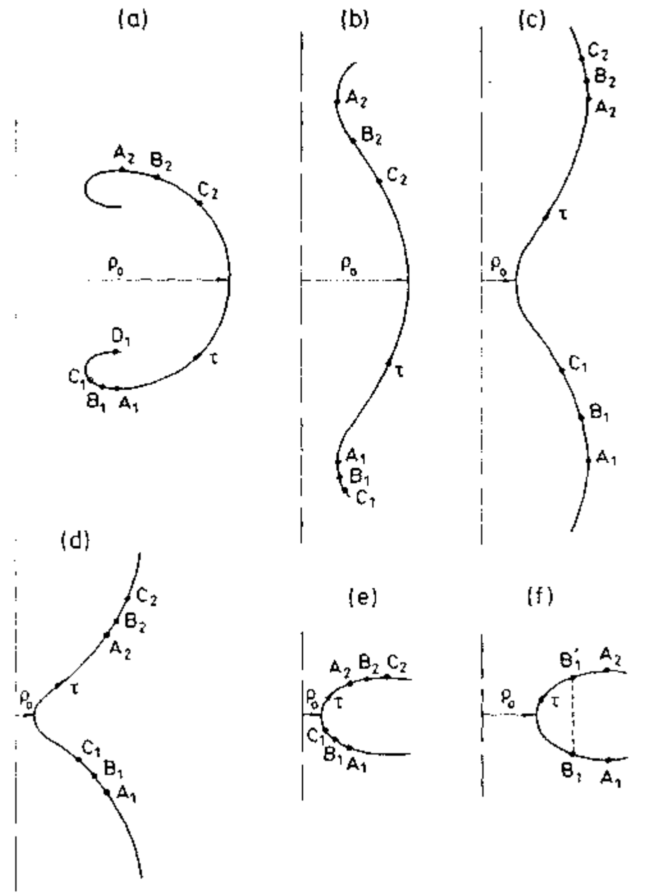

Fig. 3. Sketch of typical equilibrium shapes of liquid bridge

vanishes in the point $\tau = \tau_*^0$ is $D(\tau)$ and is critical with respect to non-axisymmetric perturbations if the function which vanishes is $\varphi_1(\tau)$. These non-axisymmetric perturbations corresponds to the first harmonic, i.e they are proportional to $\cos(\theta)$.

The constructed critical surface determines the coordinates

$$A = \frac{\zeta(\tau_*^0)}{\varrho_1^0 + \varrho(\tau_*^0)}, \quad V = \frac{4}{\zeta(\tau_*^0)[\varrho_1^0 + \varrho(\tau_*^0)]^2} \int_0^{\tau_*^0} \varrho^2 \zeta' \, d\tau \tag{3}$$

of one point of the stability boundary in the plane (A, V) for a given K. Other points can be determined in a similar way by changing the value β_1.

To better understand the numerical results, some properties of the integral lines of the system (1) [6, 7] are useful. These lines can be determined from the parameters of one of the stationary points $\tau = \tau_0$ of the function $\varrho(\tau)$ where

$$\varrho(\tau_0) = \varrho_0, \quad \varrho'(\tau_0) = 0, \quad \zeta(\tau_0) = \zeta_0, \quad \zeta'(\tau_0) = 1,$$
$$\beta(\tau_0) = \pi/2. \tag{4}$$

Since the numerical values τ_0 and ζ_0 depend only on the chosen origin of τ and on the displacement of integral line as a whole along the ζ-axis, only the value ϱ_0 is essential for characterization of the shape of integral line. This line is

Table 1. Parameters of the critical bridge belonging to upper boundary of stability region and corresponding to a change in the nature of dangerous perturbations

K	A	V	β_1	β_2	ϱ_1
0.30	0.028	15.78	−149.8	64.4	0.694
0.25	0.580	3.45	−128.3	117.9	0.576
0.20	2.138	8.46	−109.6	158.1	0.234
0.15	4.120	19.42	−104.0	167.9	0.109
0.10	7.796	52.21	−100.4	173.4	0.043

symmetric with respect to the line $\zeta = \zeta_0$ and the dependence $\varrho(\tau)$ is 2π-periodic.

3 Results

According to the above method, the calculations of the basic characteristics of the critical equilibrium states of a liquid bridge were performed for $0.1 \le K \le 0.95$ and over a wide range of A values. In the following, the obtained results are presented and their analysis in comparison with the data known for $K = 1$ [6, 7] is made.

3.1 General Boundary of Stability Region

For each value of $K < 1$, the general boundary of stability region in the plane (A, V) consists of two non-intersecting branches (upper and lower) along which $V \to \infty$ as $A \to \infty$ for both of them. The stability region spans between these branches. Fig. 2 shows the typical form of the most interesting segments of a typical boundary for $K < 1$.

3.1.1 Upper Boundary

It is determined by the critical equilibrium surfaces of nodoids with a profile which is outwards convex. The profiles of such nodoids are the portions of integral lines of the problem (1), (4) for $\beta' = 1 - \zeta'/\varrho$ and $\varrho_0 > 2$. In fig. 3a the shape of such line, corresponding to a given value of ϱ_0, is shown schematically.

Its segment A_1A_2, which is characterized by the equalities $\beta(A_1) = 0$ and $\beta(A_2) = \pi$, is the profile of the critical surface, corresponding to a certain point on upper boundary, for $K = 1$ (the designations A_1 and A_2 for the initial and the final point of the critical profile in the case $K = 1$ will also be used in the next sketches in fig. 3). It is known for such surfaces that, as A increases from zero, the value $\varrho(A_1) = \varrho(A_2) = (\varrho_0^2 - 2\varrho_0)^{1/2}$ decreases monotonically from $+\infty$ and tends to zero as $A \to \infty$; the function $V(A)$ (see dot-dash line in fig. 2) increases monotonically from 1 (the $V \cong 1 + A(\pi/2) + A^2(\frac{8}{3} - \frac{1}{4}\pi^2)$ approximation can be used for small A) and behaves as $V \sim \frac{2}{3}A^2$ as $A \to \infty$. In the case $K = 1$ the critical perturbations, which lead to neutral stability, are nonaxisymmetric and their normal to the surface component is proportional to $\zeta'(\tau)\cos(\theta)$.

The shape of the critical surfaces profiles for $K < 1$ can be inferred from fig. 3a. Let us choose as initial point on the same integral line some point B_1, in the neighbourhood of A_1, for which $\beta(B_1) < 0$. We will denote the corresponding

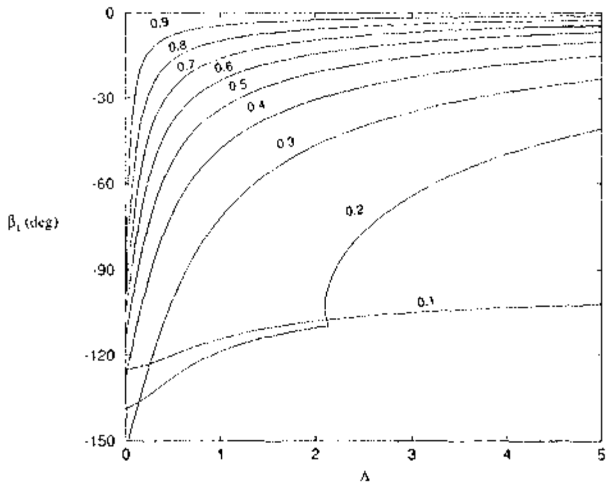

Fig. 4. Dependence of the angle at the smaller disk, β_1, on the slenderness, Λ, for critical bridges corresponding to the upper boundary of stability region. Numbers on the curves indicate the disk radii ratio, K

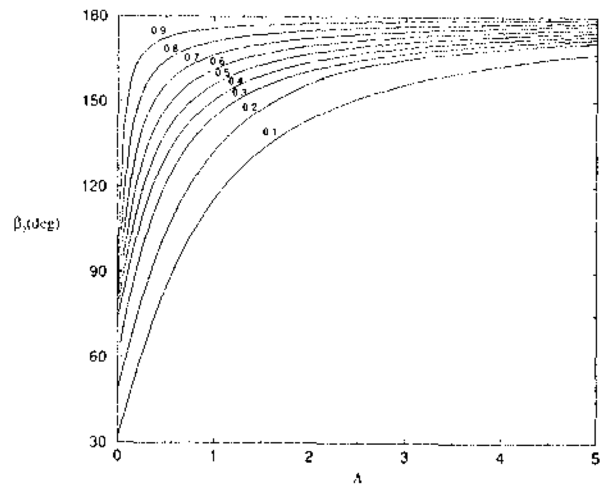

Fig. 5. Value of the angle at the larger disk, β_2, analogous to that at the smaller disk presented in fig. 4

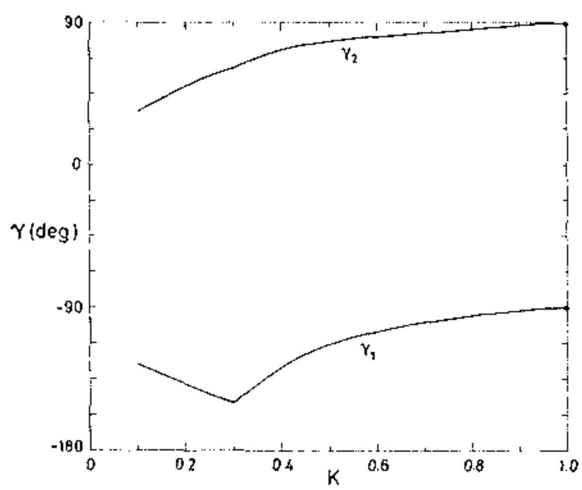

Fig. 6. Values of the minimum values of the angles at the smaller disk ($\beta_1 = \gamma_1$) and the larger disk ($\beta_2 = \gamma_2$) for critical bridges corresponding to the upper boundary and small values of the slenderness

critical point (in which either $\phi_1(\tau)$ or $D(\tau)$ vanish for the first time) by B_2. Clearly, the portion B_1B_2 cannot fully contain the portion A_1A_2, so that the point B_2 must be closely-spaced from A_2 to its lower right. The segment B_1B_2 is the profile of critical surface for $K = \varrho(B_1)/\varrho(B_2) < 1$. If the point C_1 for which $\beta(C_1) < \beta(B_1)$ is chosen as initial one, then the corresponding critical point C_2 is still further spaced from A_2 in comparison with the point B_2. Obviously, if $-\pi/2 < \beta(C_1) < 0$, the transition from the segment B_1B_2 to the segment C_1C_2 illustrates the transition of the profiles of critical surfaces with decreasing value of K.

For the initial point D_1 in which $\beta(D_1) = -\pi$, the corresponding critical point coincides with A_1. Therefore, taking into account the condition $\Lambda > 0$ ($\zeta_2 > \zeta_1$), we obtain that $-\pi < \beta_1 < 0$ and $0 < \beta_2 < \pi$ for the profile of critical surface in the case $K < 1$.

Besides, for the critical surface, as for any other equilibrium shape, the following relationship between the parameters of the initial and final points holds

$$\sin(\beta_2) = K \sin(\beta_1) + \frac{1-K^2}{2K}\varrho_1, \tag{5}$$

and the shape of the integral line is determined from the values of ϱ_1 and β_1

$$\varrho_0 = 1 + \sqrt{1 + \varrho_1^2 - 2\varrho_1 \sin(\beta_1)}. \tag{6}$$

Eqs. (5) and (6) are obtained by integrating the product of ϱ and eq. (1b) in view of the equality $\beta' = 1 - \zeta'/\varrho$.

Since the value of ϱ at the nearest to the ζ-axis stationary point of the function $\varrho(\tau)$ equals to $\varrho_0 - 2$, the given integral line can determine the profiles of a bridge only for $K \geq (1 - 2/\varrho_0)$. That is why the value ϱ_0 decreases as K decreases and $\varrho_0 \to 2^+$ as $K \to 0$.

Since for $K = 1$ the profiles of the critical surfaces are characterized by the value $\beta_1 = 0$ and in this case the non-axisymmetric perturbations are always the critical ones, it should be expected that in the case $K < 1$ for the critical surfaces, whose profiles have $|\beta_1| \ll 1$, the non-axisymmetric perturbations are still the critical ones. The probability of stability losing with respect to axisymmetric perturbations increases as $|\beta_1|$ increases. The analysis of the results, obtained for the case $K = 1$, shows that only on the integral lines corresponding to small values of $(\varrho_0 - 2)$ there are the portions which define for $K < 1$ the profiles of the surfaces critical with respect to axisymmetric perturbations.

Calculations show that for $0.307 \leq K \leq 1$ the non-axisymmetric perturbations are the critical ones in the whole upper boundary. If $0 < K < 0.306$, there is a transition value $\beta_1 = \beta_{1t}$ such that the axisymmetric perturbations are critical for $\beta_1 < \beta_{1t}$ and the non-axisymmetric ones are critical for $\beta_1 > \beta_{1t}$. The values of the parameters of critical surfaces corresponding to a change in the nature of critical perturbations are given in table 1 for different values $K < K_t$ ($0.306 < K_t < 0.307$). It should be noted that $\beta_{1t} < -\pi/2$ for all considered values of K.

The numerical results show that, along the boundary corresponding to $K = const.$ ($K_t < K < 1$), the functions

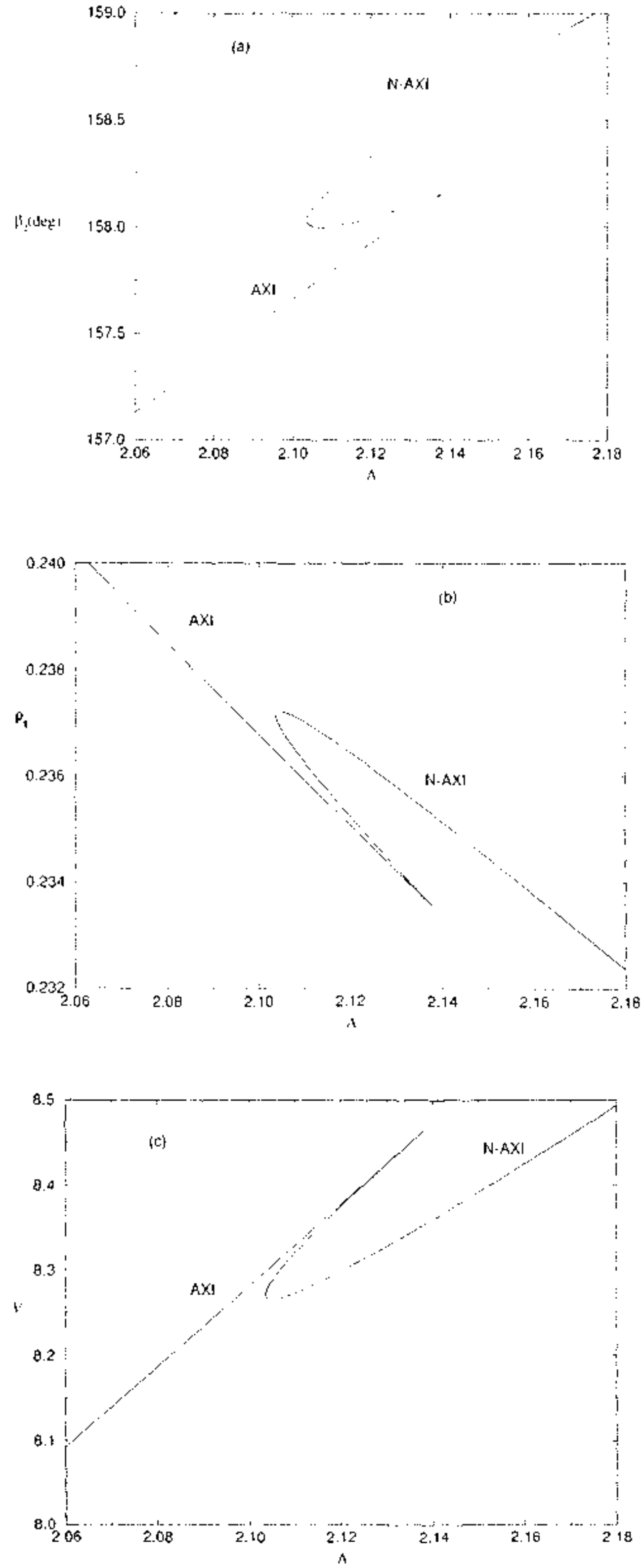

Fig. 7. Values of the angle β_2 at the larger disk (a), the dimensionless smaller disk radius ϱ_1(b) and the relative liquid volume V(c) depending on slenderness, Λ, along the upper boundary for $K = 0.2$ in the vicinity of the point of a change in the nature of critical perturbations. Labels "AXI" and "N-AXI" correspond to critical axisymmetric and non-axisymmetric perturbations, respectively

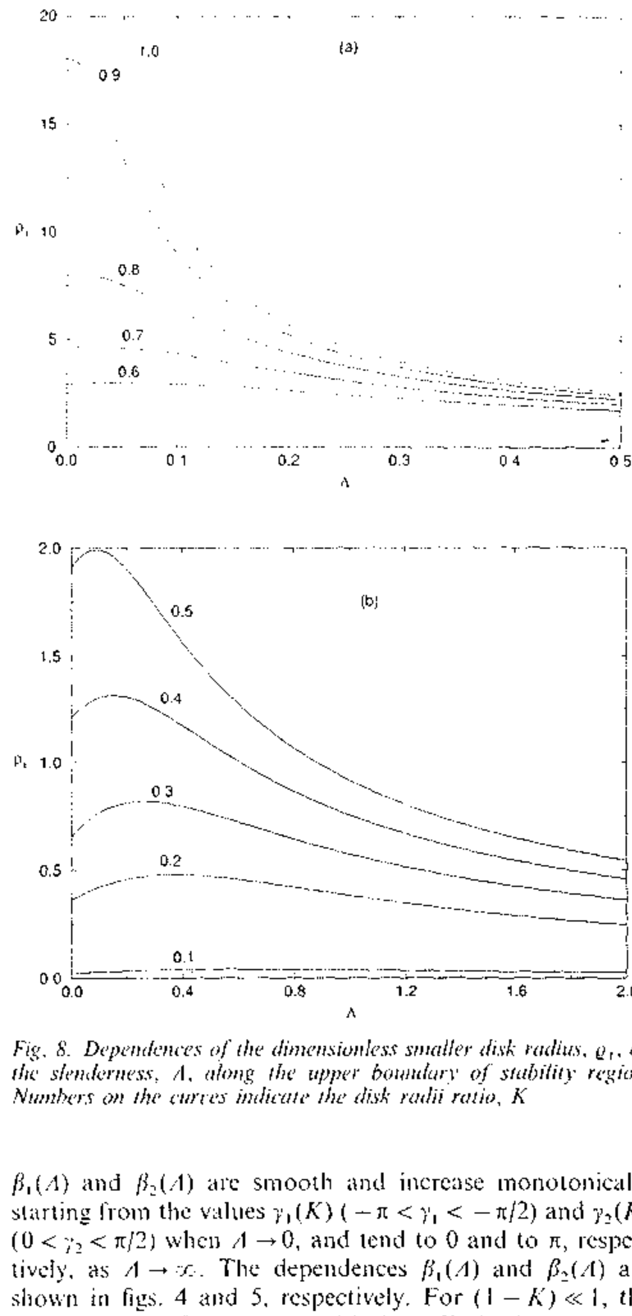

Fig. 8. Dependences of the dimensionless smaller disk radius, ϱ_1, on the slenderness, Λ, along the upper boundary of stability region. Numbers on the curves indicate the disk radii ratio, K

$\beta_1(\Lambda)$ and $\beta_2(\Lambda)$ are smooth and increase monotonically starting from the values $\gamma_1(K)$ $(-\pi < \gamma_1 < -\pi/2)$ and $\gamma_2(K)$ $(0 < \gamma_2 < \pi/2)$ when $\Lambda \to 0$, and tend to 0 and to π, respectively, as $\Lambda \to \infty$. The dependences $\beta_1(\Lambda)$ and $\beta_2(\Lambda)$ are shown in figs. 4 and 5, respectively. For $(1 - K) \ll 1$, the difference $\beta_2 - \beta_1$ on every critical profile is close to π, in agreement with eq. (5) (according to numerical results, $\beta_2 - \beta_1 = \pi + \delta$, where $0 < \delta < 0.05$ for $K \geq 0.7$, $0 < \delta < 0.02$ for $K \geq 0.8$ and $0 < \delta < 0.005$ for $K \geq 0.9$). The dependences $\gamma_1(K)$ and $\gamma_2(K)$ are shown in fig. 6. Here $\gamma_1(K) \to -\pi/2$ and $\gamma_2(K) \to \pi/2$ as $K \to 1$, although $\gamma_1 = 0$ and $\gamma_2 = \pi$ for $K = 1$.

If $0 < K < K_c$ in the point of change in the type of critical perturbations the behaviour is not smooth and in its neighbourhood the dependences $\beta_1(\Lambda)$ and $\beta_2(\Lambda)$ may be multiple-valued (for $K = 0.2$, it is illustrated in figs. 4 and 7a).

Along the upper boundary corresponding to $K = const.$, the maximum value of $\varrho_1(\Lambda)$ is obtained for a relatively small value of Λ (fig. 8) and $\varrho_1 \to 0$ as $\Lambda \to \infty$. This maxi-

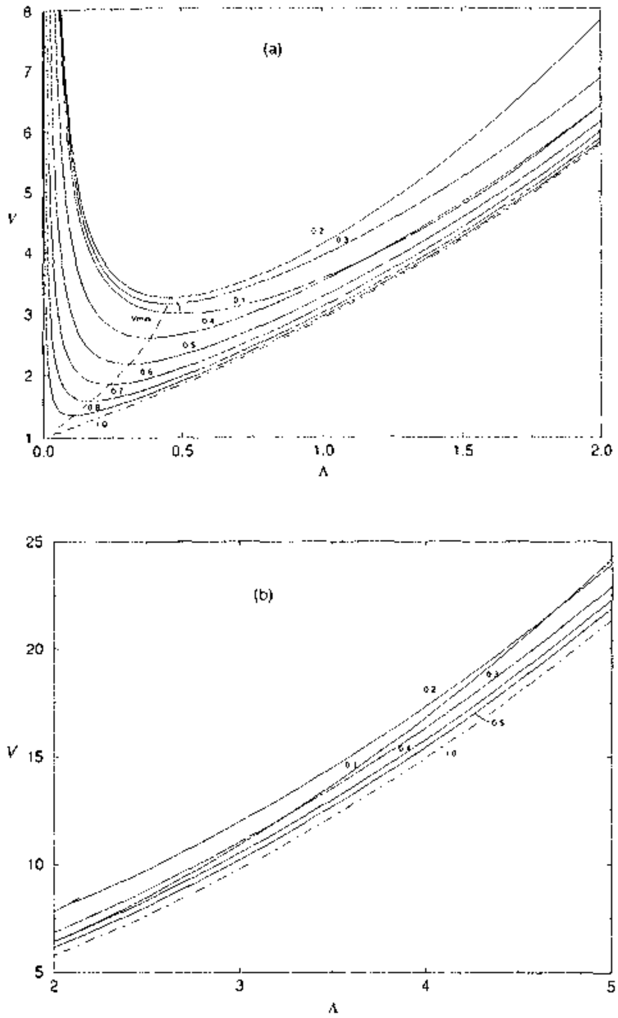

Fig. 9. Upper boundaries of stability region for small and middle (a) and large (b) values of the slenderness, A, and different values of disk radii ratio, K. Numbers on the curves indicate the values of K. The dotted line in (a) joins the points of minimum V for given K

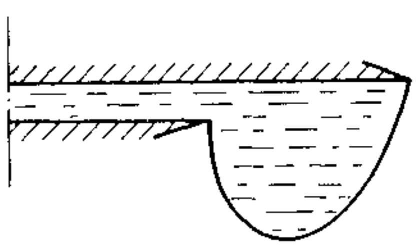

Fig. 10. Sketch of a critical equilibrium state corresponding to the maximum volume stability limit for small values of the slenderness

mum corresponds to the critical profile, for which the initial and final points are located in the immediate vicinity of the extreme points of the function $\varrho(\tau)$, so that $\varrho_1 \approx \varrho_0 - 2$, $\varrho_2 \approx \varrho_0$ and $\varrho_{1max} \approx 2K/(1-K)$ for given K. The greater K, the better is this approximation. If $0 < K < K_t$, the function $\varrho_1(A)$ loses its smoothness in the point of type change of critical perturbations and may become multiple-valued in a vicinity of this point (see fig. 7b). The dependences $\beta_1(A)$,

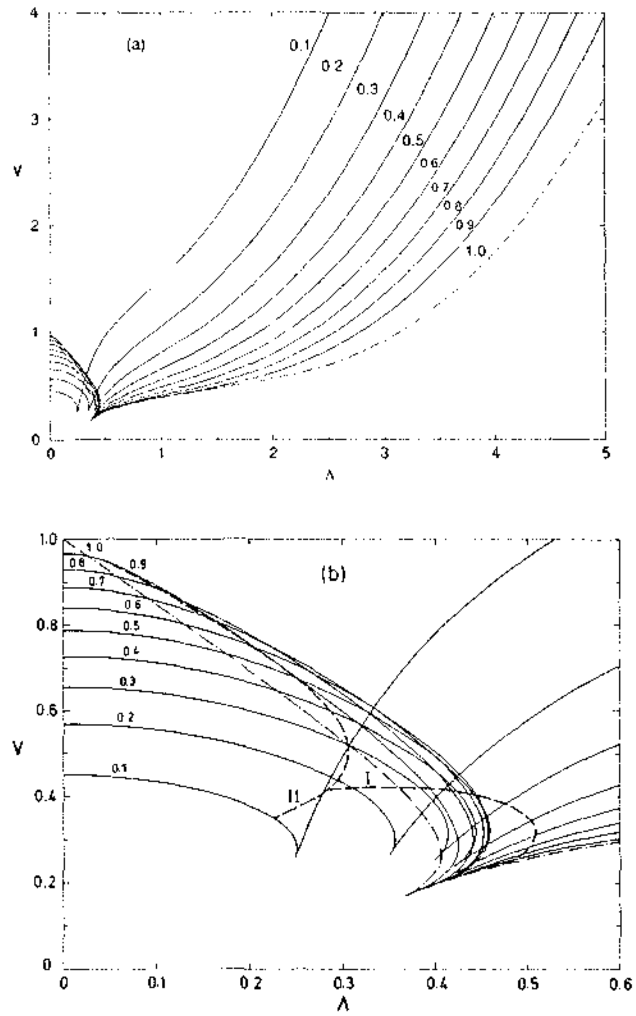

Fig. 11. Lower boundaries of stability region for various values of disk radii ratio, K, indicated by the numbers on the curves: (a) general diagram; (b) detail for small values of the slenderness, A. The dashed lines I and II are the locii of the points corresponding to the critical catenoids and the limiting nodoids with an angle $\beta_1 = \pi/2$ at the smaller disk, respectively

$\beta_2(A)$ and $\varrho_1(A)$ are connected through the relation (5) and thus they are not independent.

The parameters β_1, β_2, and ϱ_1 define the shape of surface profile, whereas A and V determine the stability of a liquid bridge for given K. A remarkable difference with the case $K = 1$ is that for $K < 1$ the dependence $V(A)$ along the upper boundary in non-monotonic: V tends to infinity not only as $A \to \infty$ but also as $A \to 0$ (see fig. 9a where the boundary segments corresponding to small values of A are presented in more detail). This behaviour can be explained from the sketch in fig. 10 (for small values of A) and from eq. (3) for V (the integral appearing in this expression remains finite as $A \to 0$).

If $A \ll 1$ and $(1 - K) \ll 1$, then the corresponding values of ϱ_1 are large (fig. 8a) and the equilibrium problem is similar to the corresponding plane problem. According to [7], in this case the profile of the critical surface is close to a semicircle and the critical perturbations are non-axisymmetric. Assuming that the profile of critical surface is a semicircle, we get

$$V = \frac{\pi(1-K)^2}{2(1+K)^2\Lambda} + \frac{2(1+K^2)}{(1+K)^2} + \frac{\pi}{2}\Lambda + \frac{2}{3}\Lambda^2. \tag{7}$$

The comparison with numerical results shows that the relative error of the approximation (7) for $K \geq 0.8$ does not exceed 1 %, if $\Lambda \leq 0.15$, and 5 %, if $\Lambda \leq 0.5$.

The dotted line in fig. 9a is the locus of the points with a minimum in the function $V(\Lambda)$, for a given K. Using eq. (7), we obtain the following coordinates of this point for $(1-K) \ll 1$:

$$\Lambda \cong \frac{1-K}{1+K} - \frac{4}{3\pi}\frac{(1-K)^2}{(1+K)^2}, \tag{8}$$

$$V \cong \frac{2(1+K^2)}{(1+K)^2} + \frac{\pi(1-K)}{(1+K)} + \frac{2}{3}\frac{(1-K)^2}{(1+K)^2}. \tag{9}$$

The relative error of these expressions is less than 1 % for $K \geq 0.9$ and less than 5 % for $K \geq 0.7$.

For $K_t \leq K \leq 1$, the upper boundary displaces upwards as the value of K decreases. The same tendency holds for $0 < K < K_t$ and the values of Λ where the nonaxisymmetric perturbations are critical. However, for values of Λ corresponding to the axisymmetric critical perturbations, the decreasing of K can cause the opposite effect (see fig. 9). The behaviour of the dependence $V(\Lambda)$ for $0 < K < K_t$ in the vicinity of the point of change in the nature of critical perturbations is illustrated in fig. 7c.

3.1.2 Lower Boundary

In the case $K = 1$ the lower boundary consists of several segments (fig. 2). The points belonging to the segments Fn ($\Lambda > \pi$) and EF ($2.130 \leq \Lambda < \pi$) correspond to unduloidal surfaces whose profiles have vertical tangents at the terminal points ($\beta_1 = \beta_2 = \pi/2$). These profiles, schematically shown in figs. 3b, c respectively, represent portions of the integral lines of the problem (1), (4) under $\beta' = 1 - \zeta'/\varrho$ and for values $1 < \varrho_0 < 2$ and $0.589 \leq \varrho_0 < 1$ respectively. In these cases the values of ϱ at the disks are $\varrho_1 = \varrho_2 = 2 - \varrho_0$. The boundary point F corresponds to the critical cylindrical surface ($\Lambda = \pi$, $\varrho_0 = 1$). The points in the segments DE ($0.472 < \Lambda < 2.130$) and CD ($0.361 < \Lambda < 0.472$) correspond to critical unduloidal surfaces and critical nodoidal surfaces respectively, whose profiles do not contain points, except the equatorial one, with a vertical or a horizontal tangent, so that $\pi/2 < \beta_1 < \pi$ and $0 < \beta_2 < \pi/2$ (see figs. 3d, e). These profiles are portions of the integral lines of the problem (1), (4), respectively, for $\beta' = 1 - \zeta'/\varrho$, $0 < \varrho_0 < 0.589$ and $\beta' = -1 - \zeta'/\varrho$, $0 < \varrho_0 < 0.095$. The boundary point D corresponds to the critical catenoidal surface. For the surfaces, corresponding to the points within the $CDEFn$ boundary segment, the axisymmetric perturbations are critical. Finally, the points belonging to the segment AC of the boundary correspond to nodoidal surfaces whose concave profiles have horizontal tangents at the terminal points ($\beta_1 = \pi$, $\beta_2 = 0$, see fig. 3f). These profiles represent portions of the integral lines of the problem (1), (4) under $\beta' = -1 - \zeta'/\varrho$, and $\varrho_0 \geq 0.095$ and here $\varrho_1 = \varrho_2 = (\varrho_0^2 + 2\varrho_0)^{1/2}$. The corresponding surfaces are critical with

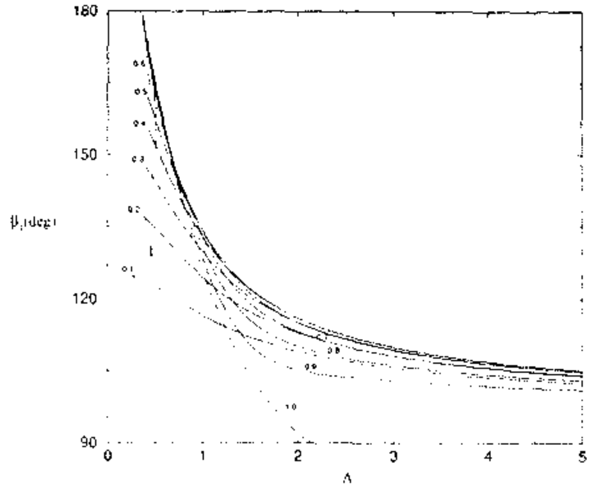

Fig. 12. Values of the angle at the smaller disk, β_1, for the critical unduloids, catenoids and nodoids determining the branches of the right-lower boundaries. The dashed line I is the locus of the points corresponding to the critical catenoids. Numbers on the curves indicate the disk radii ratio, K. The dot-dash line $K = 1$ coincides with the line $\beta_1 = 90$ for $\Lambda \geq 2.130$

respect to non-axisymmetric perturbations and, simultaneously, are the limiting ones from the point of view of the possibility of their geometrical fitting between flat disks. It should be noted that $V \sim \frac{2}{3}\Lambda^2$ as $\Lambda \to \infty$ and

$$V \cong 1 - \Lambda\frac{\pi}{2} + \Lambda^2\left(\frac{8}{3} - \frac{1}{4}\pi^2\right)$$

for small values of Λ.

Numerical results for $0.1 \leq K < 1$ have shown that all critical surfaces, for which the geometrical conditions of fitting are extrictly fulfilled ($\beta_1 < \pi$, $\beta_2 > 0$), are neutrally stable with respect to axisymmetric perturbations. Thereby, it has been confirmed the correctness of the results obtained earlier in [11], where the stability of bridges with unduloidal and catenoidal equilibrium surfaces were studied with respect to axisymmetric perturbations. The related critical surfaces correspond to the right-hand branches of the lower boundaries for given values of K (see fig. 11, where the dotted line I, separating those boundary segments, passes through the points corresponding to the critical catenoidal surfaces).

According to [5, 14], the free surface without an equatorial plane of symmetry are unstable if their profile length, $(\tau_2 - \tau_1)$, is equal to or larger than 2π. Besides, the unduloidal surface, symmetric with respect to the equatorial plane, is critical if $(\tau_2 - \tau_1) = 2\pi$ and its profile is convex in a vicinity of the equatorial point (the profile A_1A_2 in fig. 3b). Using these facts, it can be proved that, for $K < 1$, the inequalities $\pi/2 < \beta_1 < \pi$ hold for the profiles of critical unduloids. These profiles are shown schematically by segments B_1B_2 and C_1C_2 in figs. 3b–d. By considering the values ϱ_0 for the integral lines corresponding to figs. 3b–d and the properties of these lines it can be deduced that $\pi/2 < \beta_2 < \pi$ for large values of Λ (figs. 3b,c), but $0 < \beta_2 < \pi/2$ (fig. 3d) for medium values of Λ down to and including values corresponding to the critical catenoid. These statements have been confirmed by numerical results

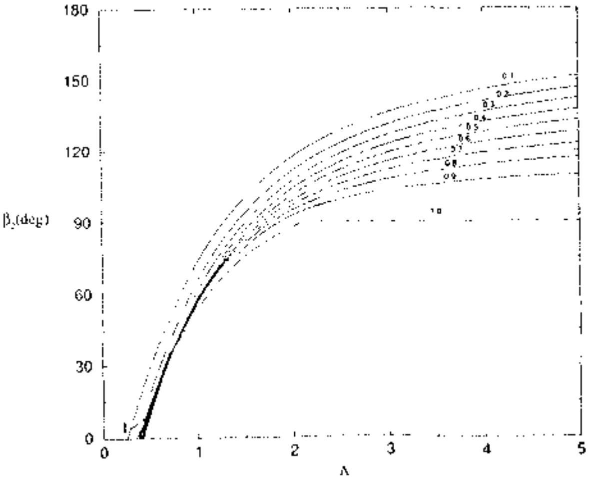

Fig. 13. Values of the angle at the larger disk, β_2, analogous to that at the smaller disk presented in fig. 12

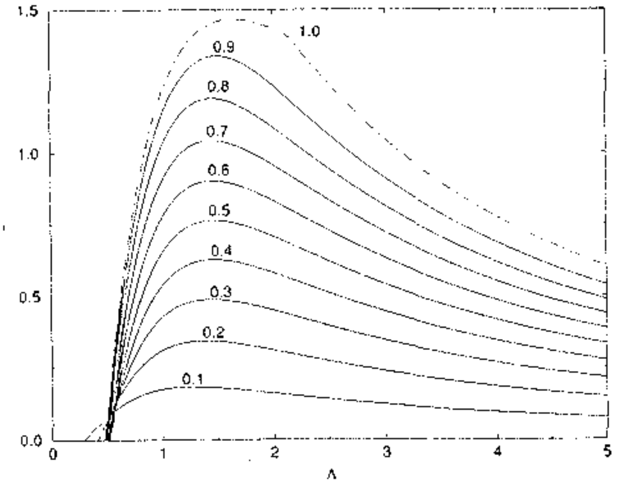

Fig. 14. Values of the dimensionless smaller disk radius, ϱ_1, depending on the slenderness, A, for the critical unduloidal surfaces. Number on the curves indicate the disk radii ratio, K

(obtained for the first time in [11]) which show in addition that, as A increases, the value β_1 along the boundary $K = const.$ decreases and β_2 increases (figs. 12, 13). The values β_1, β_2, and A for the critical catenoids related to various K were tabulated in [11]. As A increases, the quantity ϱ_1 along the branch of lower boundary $K = const.$, corresponding to critical unduloids and the critical catenoid, varies from zero (catenoid) to a maximum and then decreases tending to zero as $A \to \infty$ (fig. 14). The asymptotical behaviour of ϱ_1 as $A \to \infty$ is determined by profiles on the integral lines for which $\varrho_0 \to 2$. The equalities (5) and (6) still hold for critical unduloids and the relation $\sin(\beta_2) = K \sin(\beta_1)$ should be used instead of eq. (5) for catenoids.

Finally, it should be noted that, according to our calculations, the analytical expressions

$$V \cong \frac{2A}{\pi} - 1 + 3\left(\frac{3}{2}\right)^{1/3}\left[\frac{1-K^2}{(1+K^2)(2A - 2\sin(A))}\right]^{2/3}, \quad (10)$$

Table 2. Intervals of A values within which a relative error of eqs. (10) and (11) is smaller than indicated value

relative error (%)	K	eq. (10)	eq. (11)
1	0.9	2.95 to 3.03	2.55 to 2.95
	0.8	2.86 to 2.91	2.30 to 2.68
	0.7	2.76 to 2.80	2.12 to 2.38
2	0.9	2.90 to 3.08	2.48 to 3.04
	0.8	2.83 to 2.94	2.23 to 2.77
	0.7	2.74 to 2.82	2.03 to 2.50
5	0.9	2.73 to 3.20	2.35 to 3.24
	0.8	2.74 to 3.03	2.10 to 2.97
	0.7	2.67 to 2.89	1.88 to 2.70

$$V \cong \frac{2A}{\pi} - 1 + 3\left(\frac{3}{2}\right)^{1/3}\left[\frac{1-K}{\pi(1+K)}\right]^{2/3} \quad (11)$$

suggested by *Meseguer* [12, 13] for the approximation of the lower boundary, when $(1-K) \ll 1$ and $|A - \pi| \ll 1$, can be used with the relative error shown in table 2.

The segments of the lower boundaries, included between the intersection point (analogous to point C for $K = 1$, see fig. 2) and the dotted line I (fig. 11b), are determined by the critical nodoidal surfaces with outwards concave profiles which belong to the integral lines of the problem (1), (4) for $\beta' = -1 - \zeta'/\varrho$ and $0 < \varrho_0 < 0.095$. Schematically, they are shown in fig. 3e. For the initial point B_1, neighbouring to A_1 and such that $\beta(B_1) < \beta(A_1)$, the corresponding critical point B_2 is closely-spaced from A_2 and $\beta(B_2) < \beta(A_2)$. The profile B_1B_2 determines one of the critical nodoidal surfaces for $K = \varrho(B_1)/\varrho(B_2) < 1$. Successive displacements of the initial point in the direction of decreasing β_1 lead to the sequence of critical profiles on a given integral line with decreasing K and decreasing β_2, which is still positive. Finally, there exists some initial point C_1 for which the point C_2 with $\beta(C_2) = 0$ is critical. The profile C_1C_2 determines the critical surface which corresponds to the intersection point on the lower boundary for $K = \varrho(C_1)/\varrho(C_2)$. For the profiles of critical nodoids the inequalities $\pi/2 < \beta_1 < \pi$, $0 < \beta_2 < (\pi - \beta_1)$ hold. Corresponding dependences $\beta_1(A)$ and $\beta_2(A)$ extend the same previously constructed dependences for critical unduloids beyond the dotted line I (figs. 12, 13). The dependences $\varrho_1(A)$ are the segments of the curves presented in fig. 15 which are included between $\varrho_1 = 0$ and the intersection points on these curves. For nodoids with concave profiles, the relations

$$\sin(\beta_2) = K\sin(\beta_1) - \frac{1-K^2}{2K}\varrho_1,$$

$$\varrho_0 = -1 + \sqrt{1 + \varrho_1^2 + 2\varrho_1\sin(\beta_1)}$$

should be used instead of eqs. (5) and (6).

Choosing the initial point with a value $\beta_1 < \beta(C_1)$ on the integral line corresponding to $\beta' = -1 - \zeta'/\varrho$ and $0 < \varrho_0 < 0.095$ (fig. 3e), we will obtain $\beta_2 < 0$ for the critical profile. The same will happen for the integral lines corresponding to $\beta' = -1 - \zeta'/\varrho$ and $\varrho_0 \geq 0.095$, if we choose (necessarily) the initial point with $\beta_1 < \pi$ (fig. 3f). However, the critical nodoidal surface with $\beta_2 < 0$ does not satisfy the

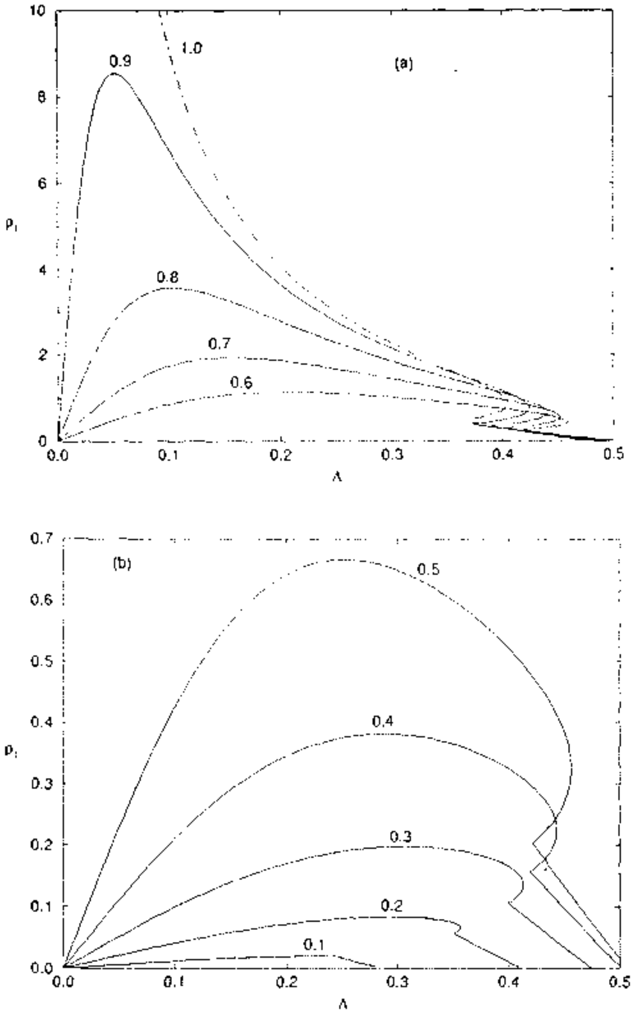

Fig. 15. Values of the dimensionless smaller disk radius, ϱ_1, depending on the slenderness, Λ, for the critical and limiting nodoid surfaces. Numbers on the curves indicate the disk radii ratio, K

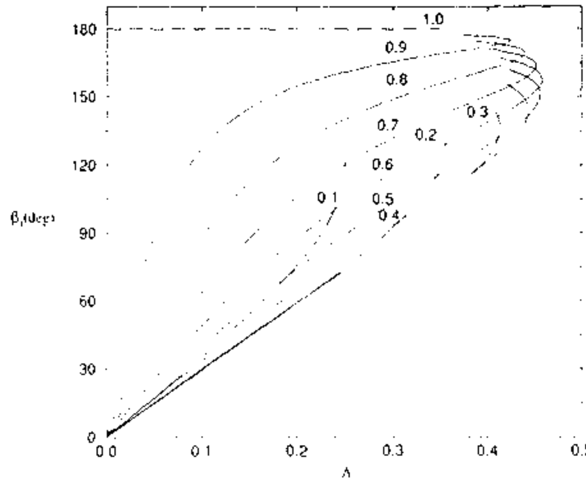

Fig. 16. Values of the angle at the smaller disk, β_1, for the limiting nodoid surfaces. Numbers on the curves indicate the disk radii ratio, K

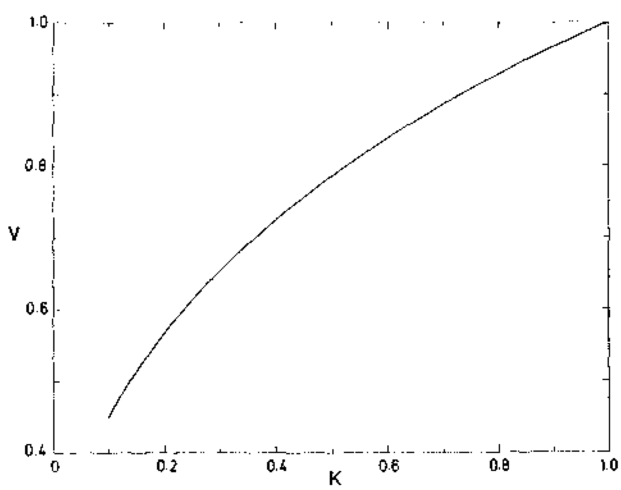

Fig. 17. Dependence of the relative liquid volume, $V = V_0$, for small values of slenderness on the disk radii ratio, K, for the limiting nodoid surfaces

geometric condition of fitting between flat solid disks. Therefore, the left-hand segment of the lower boundary included between the intersection point and the point with $\Lambda = 0$ (fig. 11b) is determined by the limiting nodoidal surfaces whose concave profiles are bounded by a final point with $\beta_2 = 0$. These surfaces are stable. But for values of the parameters Λ and V lying below and above mentioned boundary segment, there does not exist any liquid bridge equilibrium surface pinned to the edges of the disks.

When moving along this boundary segment from the intersection point, the value of β_1 is decreasing monotonically starting from the value $\beta_1 > \pi/2$ at the intersection point and tending to zero as $\Lambda \to 0$ (fig. 16). In so doing the value ϱ_1 increases initially from its value ϱ_{1B} at the intersection point to the maximum value $\varrho_{1max} = 2K^2/(1 - K^2)$ and decreases subsequently, approaching to zero as $\Lambda \to 0$ (fig. 15).

If $(1 - K) \ll 1$, for the interval of Λ values corresponding to large values of ϱ_1, the profile of the limiting nodoidal surface can be substituted for a circle arc and therefore the following approximate relationships can be obtained.

$$\cos(\beta_1) \cong \frac{(1-K)^2 - (1+K)^2\Lambda^2}{(1-K)^2 + (1+K)^2\Lambda^2},$$

$$V \cong \frac{4}{(1+K)^2(1-\cos(\beta_1))} \cdot \left\{ 1 - \cos(\beta_1) - \frac{(1-K)}{\sin(\beta_1)} (\beta_1 - \sin(\beta_1)\cos(\beta_1)) + \frac{(1-K)^2}{\sin^2(\beta_1)} \left(\frac{2}{3} - \cos(\beta_1) + \frac{1}{3}\cos^3(\beta_1) \right) \right\}. \quad (12)$$

For the profile corresponding to ϱ_{1max}, the value β_1 is $\pi/2$. The parameters of related equilibrium state

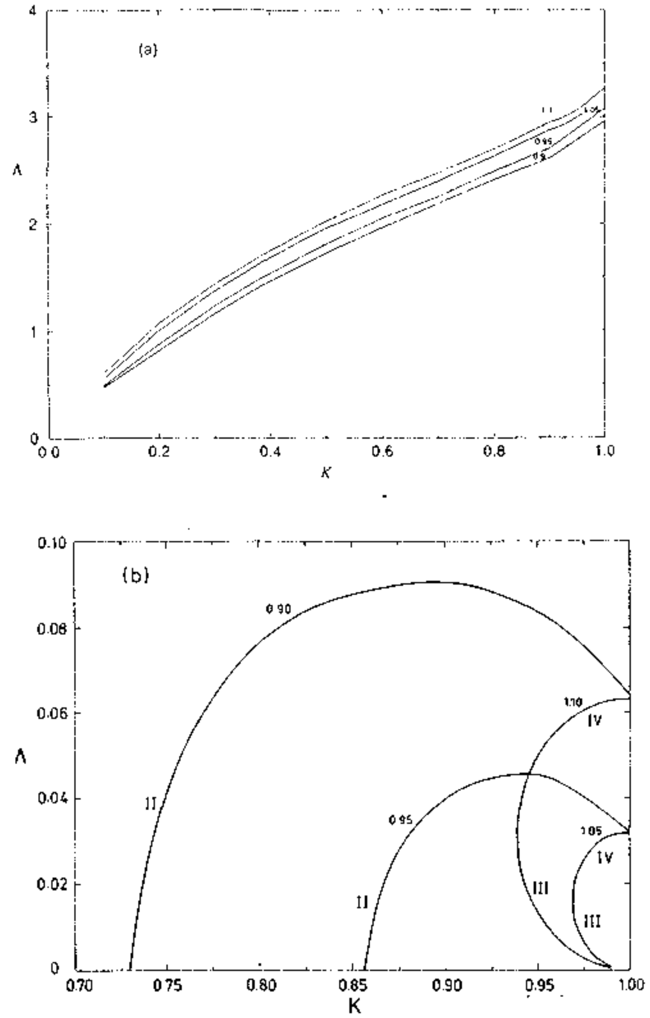

Fig. 18. Critical values of the slenderness, Λ, depending on disk radii ratio, K. Numbers on the curves indicate the relative volume, V

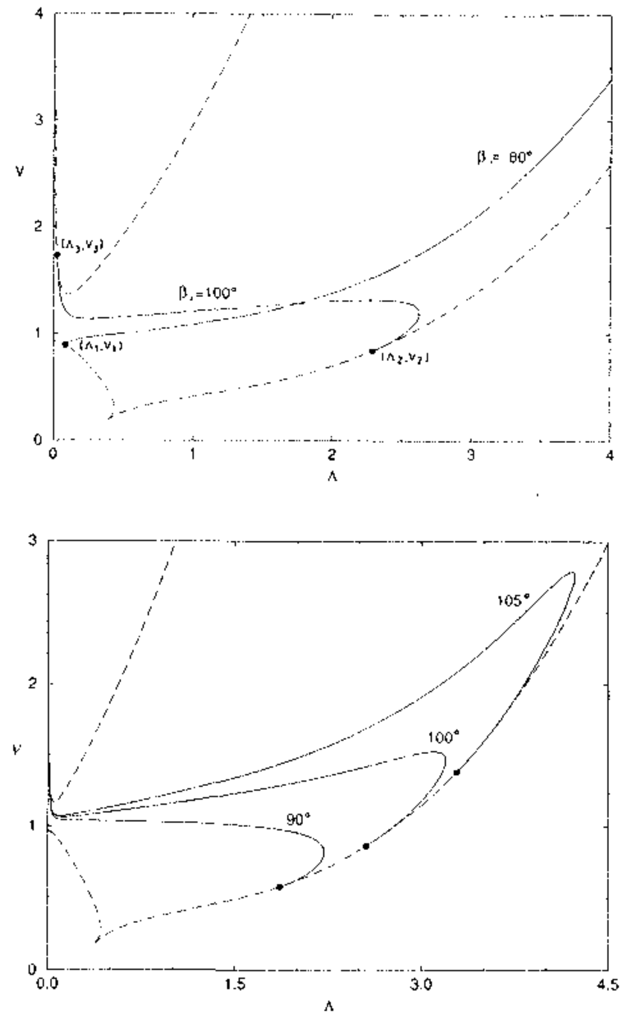

Fig. 19. Boundaries of the stability region of liquid bridges with a disk radii ratio of (a) K = 0.8 and (b) K = 0.9 (dashed lines). The solid lines correspond to given values of (a) $\beta_1 = 80$ and $\beta_2 = 100$ and (b) $\beta_1 = 90°, 100°, 105°$

$$\Lambda = \frac{1-K}{2K}\left[1 - \frac{\pi}{4}\frac{1-K^2}{2K^2} + \frac{\pi}{4}\left(\frac{1-K^2}{2K^2}\right)^2 + \cdots\right],$$

$$V = \frac{4K^2}{(1+K)^2}\left[1 + \left(2 - \frac{\pi}{2}\right)\frac{1-K^2}{2K^2} - \left(\frac{1}{2}\pi + \frac{1}{8}\pi^2 - \frac{8}{3}\right)\left(\frac{1-K^2}{2K^2}\right)^2 + \cdots\right],$$

obtained by considering a deviation of the profile from the circle arc, are more precise when compared with those following from eq. (12). Here the relative error is smaller than 0.6% if $K \geq 0.8$.

Fig. 11b shows the dashed line II which is the locus of the points corresponding to the equilibrium state with ϱ_{1max}. The other profiles of the limiting surfaces are separated into two classes: those containing the point with vertical tangent ($\pi/2 < \beta_1 < \pi$) and those not having this point ($0 < \beta_1 < \pi/2$). The profiles of these two different classes (the profiles $B_1 A_2$ and $B_1' A_2$ in fig. 3f) correspond to the same value of ϱ_1, $\varrho_{1B} < \varrho_1 < \varrho_{1max}$; the addition of the values of β_1 for these two profiles is π. The value V tends to V_0 as $\Lambda \to 0$, where $V_0 < 1$ for $K < 1$. The dependence $V_0(K)$ is shown in fig. 17.

3.2 Particular Results

Let us present in more detail some results, interesting for the floating zone technique. First of all, they are concerned to data on the stability of a liquid zone for the values of V which are close to one. In fig. 18 the dependences of the critical values of Λ on K are shown for $V = 0.9$, 0.95, 1.05, and 1.1. The dependences I (fig. 18a) correspond to the right-hand parts of the lower boundaries of stability region, the dependences II (fig. 18b) to the left-hand parts of these boundaries, and the dependences III and IV (fig. 18b), which continue each other, correspond to the left-hand and right-hand segments (they are separated by the dotted line in fig. 9a) of the upper boundaries of stability region.

If $V \leq 1$, a single interval of stable values of Λ exists for the every K. For $K \leq K_1(V)$, this interval is bounded by the line $\Lambda = 0$ and the curves corresponding to dependence I

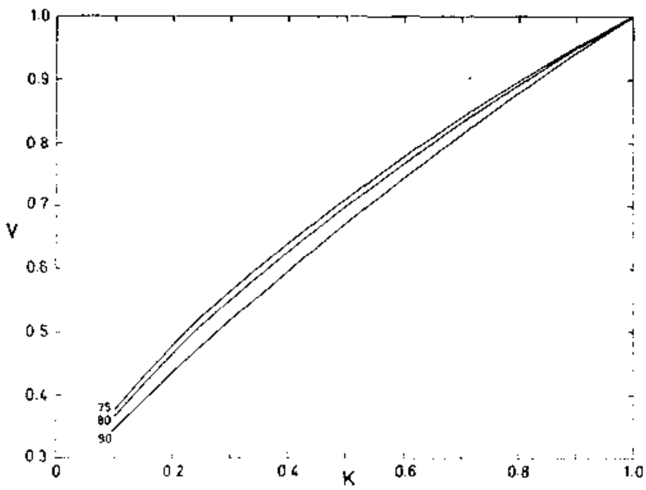

Fig. 20. Limit of minimum relative volume, V, depending on the disk radii ratio, K, for stable bridges with given values of the angle β_1 on the smaller disk. Numbers on curves indicate the values of β_1

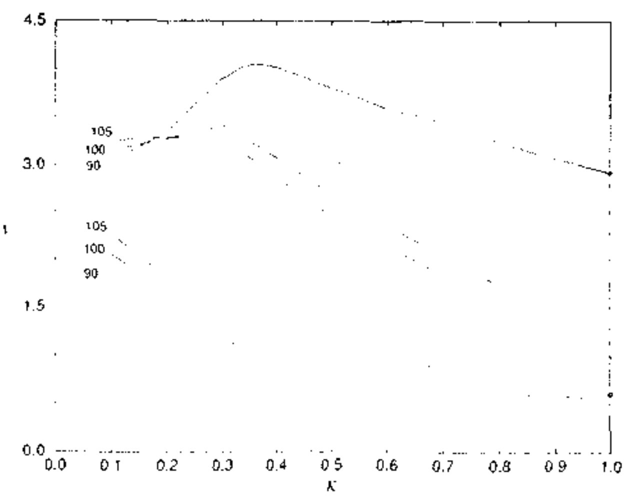

Fig. 21. Minimum and maximum values of relative liquid volume, V, for the stable bridges states with given values of the angle β_2 on the larger disk. Numbers on curves indicate the values of β_2

with given V and, for $K > K_1(V)$, by the curves corresponding to dependences II and I. The function $K = K_1(V)$ is the inverse of the function $V_0(K)$ presented in fig. 17.

If $V > 1$, then, for $K < K_2(V)$, a single interval of the above mentioned values of Λ still exists, and it is bounded by $\Lambda = 0$ and the curve corresponding to dependence I. For $K > K_2$, two intervals exist: first of them spans between $\Lambda = 0$ and the dependence III and the second one between dependences IV and I. For $K = K_2$, the lower (III) and the upper (IV) dependences merge. The values K_2 is determined as the K value for which the minimum of the function $V(\Lambda)$ on the upper boundary equals to the given value of V. It can be found from eq. (9).

Let us derive a formula, which like eqs. (7)–(12) can be used for the construction of the above mentioned dependences. It determines the relation between Λ and the critical value of V on the lower boundary in the case of $K = 1$ and $|V-1| \ll 1$. It can be obtained from the analysis of the critical shapes of unduloids which are close to the cylinder yielding

$$V \cong 1 - 2\left(\frac{\Lambda}{\pi} - 1\right) + \frac{5}{2}\left(\frac{\Lambda}{\pi} - 1\right)^2. \tag{13}$$

In this case the relationship (13) is more precise when compared with other obtained earlier [12, 13] where only the linear part of this dependence was considered.

It is preferable to carry out the crystal growth under a constant value of the growing angle α. This angle is defined as $\alpha = \pi/2 - \beta_1$ or $\alpha = \beta_2 - \pi/2$ depending on whether the solidification front is considered to be the smaller or the larger disk. The value α depends on the physical properties of the solid material and, usually, is close to zero but for single crystals of Si and Ge it turns to be equal to $11 \pm 1°$ and $13 \pm 1°$, respectively [15]. Therefore the data of main interest are those on the stability of a bridge for $\beta_1 = 90°, 80°, 75°$ and $\beta_2 = 90°, 100°, 105°$.

According to the results presented in sect. 3.1, the equilibrium bridge surfaces are stable for $K < 1$ and $0 \le \beta_1 \le \pi/2$ if they satisfy the geometric condition of fitting ($\beta_2 \ge 0$) and have not any neck ($\tau_2 - \tau_1 < 2\pi$). In the (Λ, V)-plane, the line corresponding to the above states with a given value of β_1 starts in some point (Λ_1, V_1) on the left-hand part of the lower boundary and no longer crosses the boundary but lies inside the stability region corresponding to K. Along this line, $\Lambda \ge \Lambda_1$, and $V(\Lambda)$ is a monotonically increasing function (fig. 19a). The stability boundary for such states is determined by the minimum volume value ($V = V_1$) which is necessary for the fulfillment of the fitting condition. For the above mentioned values of β_1, it is presented in fig. 20.

The line corresponding to the stable equilibrium states with given $\beta_2 \ge \pi/2$ lies inside the stability region for the related K and joins some points (Λ_3, V_3) and (Λ_2, V_2) on the upper boundary and on the right-hand part of the lower boundary respectively (fig. 19a). Along this line both the Λ and V values can vary non-monotonically reaching the minimum and the maximum value of V and the maximum value of Λ inside the stable region. Such behaviour of the quantities Λ and V is typical for the relatively large values of K and not-too-small values of ($\beta_2 - \pi/2$) (see fig. 19). Therefore, the stability of these states is not uniquely determined by the parameters (Λ_2, V_2) and (Λ_3, V_3) of the critical states. An unambiguous conclusion on the stability can be made only for the values of K for which the V values along the line $\beta_2 = const.$ satisfy the unequalities $V_2 < V < V_3$ inside the stable region. For these values of K the minimum, V_2, and the maximum, V_3, values of V for the stable states under the above mentioned values of β_2 are given in fig. 21.

4 Conclusions

Some numerical results and approximate formulas are presented which allow to judge on the stability or instability of axisymmetric equilibrium states of a zero-g liquid bridge between unequal disks for given values of radii of disks, their separation and liquid volume. It has been found that disk radii inequality leads to a qualitative change in the form of the stable region boundary.

Acknowledgments

This work has been supported by the Spanish Comisión Interministerial de Ciencia y Tecnología (CICYT) and is part of a more general endeavour for the study of fluid physics and materials processing under microgravity (Project No. ESP92-0001-CP). One of the authors, L.A.S., has been supported by the Spanish Dirección General de Investigación Científica y Técnica (DGICYT) Project No. SAB93-0008.

References

1 *Wilker, K.-Th.:* Kristallzüchtung, DVdW, Berlin (1973)
2 *Steg, L.* (ed.): Materials Sciences in Space with Application to Space Processing, Amer. Inst. Aeronaut. Astronaut., New York (1977)
3 *Plateau, J.:* Statique Expérimentale et Théorique des Liquides Soumis aux Seules Forces Moléculaires, Gauthier-Villars, Paris (1873)
4 *Micheal, D. H.:* Meniscus Stability. Ann. Rev. Fluid Mech., vol. 13, p. 189 (1981)
5 *Gillette, R. D., Dyson, D. C.:* Stability of Fluid Interfaces of Revolution Between Equal Solid Circular Plates. Chem. Eng. J., vol. 2, p. 44 (1971)
6 *Slobozhanin, L. A.:* Problems of the Stability of Liquids in Equilibrium, Appearing in Spatial Technology; in Hydromechanics and Heat and Mass Transfer in Zero-gravity, p. 9, Nauka, Moscow (1982) (in Russian)
7 *Myshkis, A. D., Babskii, V. G., Kopachevskii, N. D., Slobozhanin, L. A., Tyuptsov, A. D.:* Low-gravity Fluid Mechanics, Springer-Verlag, Berlin (1987)
8 *Sanz, A., Martínez, I.:* Minimum Volume for a Liquid Bridge Between Equal Disks. J. Coll. Interface Sci., vol. 93, p. 235 (1983)
9 *Russo, M. J., Steen, P. H.:* Instability of Rotund Capillary Bridges to General Disturbances – Experiment and Theory. J. Coll. Interface Sci., vol. 113, p. 154 (1986)
10 *Martinez, I.:* Stability of Axisymmetric Liquid Bridges; in: ESA SP-191, p. 267, European Space Agency, Paris (1983)
11 *Martinez, I., Perales, J. M.:* Liquid Bridge Stability Data. J. Cryst. Growth, vol. 78, p. 369 (1986)
12 *Meseguer, J.:* Stability of Long Liquid Columns; in: ESA SP-222, p. 297, European Space Agency, Paris (1984)
13 *Meseguer, J.:* The Dynamics of Axisymmetric Slender Liquid Bridges Between Unequal Disks. J. Cryst. Growth, vol. 73, p. 599 (1985)
14 *Slobozhanin, L. A.:* Hydrostatic Problems Arising during Simulation of the Process of Purification of Materials and Growth of Single Crystals by the Floating Zone Method. Part 2. Equilibrium and Stability of Zone Melt under Zero-gravity Condition. Preprint 24-84, Fiz. Tekh. Inst. Nizk. Temp. Akad. Nauk Ukr. SSR, Kharkov (1984) (in Russian)
15 *Surek, T., Coriell, S. R.:* Shape Stability in Float Zoning of Silicon Crystals. J. Cryst. Growth, vol. 37, p. 253 (1977)